Research Square

Preprints are preliminary reports that have not undergone peer review.
They should not be considered conclusive, used to inform clinical practice,
or referenced by the media as validated information.

Lactobacillus plantarum RLL68 fermented black tea beverage attenuates high-fat-diet-induced non-alcoholic fatty liver by modulating hepatic lipid metabolism and gut microbiota

Ruili Li
Fujian Polytechnic Normal University
Chong Xu
Anhui New Simon Biotechnology Co., LTD
Yifei Lu
Anhui New Simon Biotechnology Co., LTD
Anxin Sun
Anhui New Simon Biotechnology Co., LTD
Xinghu Lu
Anhui New Simon Biotechnology Co., LTD
Yifeng Liu
Fujian Agriculture and Forestry University
Jinzhi Han
hjz419@fzu.edu.cn

Fuzhou University

Research Article

Keywords: Fermented black tea beverage, Lactobacillus plantarum RLL 68, Fatty liver, High-fat diet, Gut microbiota, Lipid metabolism

Posted Date: September 23rd, 2026

DOI: https://doi.org/10.21203/rs.3.rs-10806318/v1

License: This work is licensed under a Creative Commons Attribution 4.0 International License.
Read Full License

Additional Declarations: No competing interests reported.

Abstract

Lactic acid bacteria (LAB)-fermented foods possess prominent gastrointestinal regulatory functions and excellent physiological nutritional value. This study aimed to investigate the ameliorative effects of *L. plantarum* RLL68-fermented black tea beverage (FBTB) on high-fat diet (HFD)-induced non-alcoholic fatty liver (NAFL) in mice. The results demonstrated that FBTB intervention significantly mitigated the elevation of serum lipid indicators, including total cholesterol, triglycerides, and low-density lipoprotein cholesterol (LDL-c), and effectively alleviated excessive hepatic lipid accumulation. Moreover, FBTB improved glyceride and glycerophospholipid metabolism by upregulating the levels of hepatoprotective unsaturated lipids and phospholipids, while reducing the abundance of lipogenic saturated lipids that drive hepatic steatosis. Additionally, FBTB supplementation improved gut microbial diversity in HFD-fed mice, remarkably enriched beneficial bacterial genera such as *Lactobacillus*, *Akkermansia*, and *Dubosiella*, and suppressed the proliferation of steatosis-associated detrimental taxa including *Alistipes* and *Bacteroides*. Correlation analysis verified that *Lactobacillus* and *Akkermansia* were positively correlated with unsaturated lipid contents and negatively correlated with saturated lipid levels. Collectively, two-month FBTB intervention effectively reshaped the gut microbiota structure and promoted short-chain fatty acid (SCFA) production in mice. Furthermore, FBTB synergistically modulated the expression of lipid metabolism-related genes (e.g.,Acaca, Cpt1a) and functional proteins (TLR4, ALDH2), thereby restoring disrupted hepatic lipid homeostasis. In conclusion, FBTB exerts protective effects against HFD-induced NAFL via regulating gut microbiota and hepatic lipid metabolism. This finding provides a theoretical basis for the development and application of LAB-fermented functional foods for the prevention and improvement of NAFL and related metabolic disorders.

1. Introduction

The prevalence of non-alcoholic fatty liver (NAFL) has escalated in recent years, emerging as a prominent etiology for liver cirrhosis and hepatocellular carcinoma, thereby posing a considerable threat to public health[1]. NAFL is characterized by abnormal accumulation of lipids in the liver[2]. It is closely associated with a range of metabolic disorders, such as obesity, insulin resistance, dyslipidemia, and steatohepatitis[3]. Current pharmacological interventions for NAFL include insulin sensitizers, antioxidants, lipid-lowering and/or weight-reducing agents, as well as hepatoprotective drugs[4]. Although these medications offer rapid onset and significant efficacy in treating NAFL, they can also induce adverse reactions such as gastrointestinal discomfort and indigestion. Additionally, concomitant use of multiple drugs may lead to hepatic failure[5]. Prevention and adjunctive therapy of NAFL using plant-derived natural products and functional foods have long been fundamental principles in traditional Chinese medicine [6]. The potential of tea for preventing and ameliorating various ailments, including obesity and NAFL, renders it a promising dietary intervention for the prevention and management of NAFL[7].

The LAB, such as *Lactobacillus plantarum*, *Lactobacillus casei*, *Lactobacillus rhamnosus*, and *Bifidobacterium adolescentis*, are classified as GRAS (Generally Recognized as Safe) microorganisms

and represent the predominant bacterial species in most fermented foods[8]. Additionally, LAB fermentation not only imparts desirable flavors to fermented foods, but also provides postbiotic such as organic acids, active peptides, exopolysaccharides[9–11]. Therefore, the fermented foods produced using LAB enhances their nutritional value and health-promoting properties by improving gastrointestinal function, reducing serum lipids, and alleviating obesity and NAFL[12, 13]. For instance, *L. plantarum* can mitigate the progression of NAFL through modulating gut microbiota, improving metabolic risk factors, and attenuating adipose inflammation of mice[14]. In addition, the anti-inflammatory properties of *L. acidophilus*, along with its ability to alleviate endothelial dysfunction and gut dysbiosis, make it a promising candidate for probiotic therapy in the management of obesity and related conditions such as hyperlipidemia, NAFL, and insulin resistance[15]. Moreover, *B. adolescentis* and *L. rhamnosus* can inhibit the progression of NAFL in mice by regulating gut microbiota[16].

Currently, a wealth of evidence suggests that the gut microbiota plays a pivotal role in both the pathogenesis and progression of NAFL and its more severe manifestation, nonalcoholic steatohepatitis (NASH)[17]. It was indicated that targeting the gut microbiota represents a promising therapeutic approach for both prevention and amelioration of NAFL. The gut-liver axis is the pathophysiological basis for therapy of liver disease and represents a bidirectional interplay between the gastrointestinal tract, its commensal microbiota, and the hepatic system[18]. This intricate crosstalk is modulated by various factors including dietary habits, genetic predisposition, and environmental cues; while the portal vein serves as a conduit for direct transfer of luminal contents from the gut to the liver, feedback loops are established through bile secretion and immunoglobulin production targeting intestinal antigens; the intestinal barrier serves as a formidable defense against the invasion of harmful microbes and toxins, while simultaneously facilitating the transportation of vital nutrients to the liver. Moreover, the preservation of gut microbial communities is paramount for maintaining optimal gut-liver axis homeostasis, which is achieved through reciprocal communication that shapes these communities[19].

In our previous study, the strain of *L. plantarum* RLL 68, previously isolated from Chinese sauerkraut, was employed to ferment black tea beverage. The FBTB exhibits elevated levels of various organic acids, including lactic acid, acetic acid, citric acid and succinic acid, as well as γ-aminobutyric[20]. In this study, a high-fat diet (HFD) induced non-alcoholic fatty liver (NAFL) mouse model was established, with phenotypic confirmation of hepatic steatosis via histological and biochemical analyses. Leveraging multi-omic approaches including 16S rRNA sequencing of the gut microbiota and targeted lipidomics of hepatic tissues the investigation unraveled the molecular mechanisms by which the *L. plantarum* RLL68 fermented black tea beverage mitigates NAFL. These findings not only delineate the mechanism of action but also posit the fermented beverage as a promising dietary intervention for preventing and managing NAFL.

2. Materials and methods

2.1 Preparation of fermented black tea beverage

The fermented black tea beverage was prepared following the previously described procedure[20]. As shown in Fig. 1, the strain of *L. plantarum* RLL 68 was inoculated to liquid MRS medium and statically cultured at 37 ℃ until it reached the exponential growth phase. The bacterial cells were then harvested by centrifugation at 4 ℃ and 8000 g for 5 min, followed by resuspension in fresh sterilized water to achieve an optical density of 0.6 at 600 nm (10^8 CFU/mL). Additionally, 60 g of black tea was infused in 6 L of boiling water for 5 min, and the supernatant was collected by filtration through gauze. Subsequently, 60 g of glucose was added to the tea infusion, which was then sterilized at 115 ℃ for 15 min. The sterilized black tea soup was then inoculated with 1% of the previously prepared bacterial suspension and subjected to static fermentation at 37 ℃ for 72 h until the pH of the supernatant reached 4.0. Subsequently, the beverage was treated at 85°C for 25 min and then stored at 4°C. A non-fermented black tea beverage was also produced following the same protocol, excluding the fermentation step. The main ingredients of the fermented and non-fermented black tea beverage are presented in Table S1.

2.2 Animal experiment design

The animal experiments were carried out in accordance with the Guidelines of the National Research Council (1996) and complied with the regulations set by the Ethics and Animal Welfare Committee, China (revised 2016). The animal experiments were approved by the Institutional Ethical Committee of Animal Experimentation of the Fuzhou University (Ethical Permit No: 2022-SG-026). The establishment of NAFL mouse model induced by high-fat diet was performed following a previously described methodology[21]. The ICR (Kunming) male mice used in this study were purchased from Fuzhou Wu's Experimental Animal Trade Co., Ltd. (Fuzhou, China). The mice were 6-week-old with body weights ranging from 20 to 25 g upon arrival.The mice were housed in a temperature-controlled environment (temperature of 18 ~ 20 ℃ and humidity of 50 ~ 60%) with a 12-hour light-dark cycle and provided ad libitum access to sterile water and standard chow. After one week of acclimation, the animals were randomly assigned to 5 groups, each consisting of eight individuals, and provided with distinct diets as follows: (i) normal diet group (NFD), fed with a normal diet (10% kcal energy from fat, Wu's Experimental Animal Trade Co., Ltd., Fuzhou city, China) and sterile water; (ii) high-fat diet group (HFD), fed with a high-fat diet (45% kcal energy from fat, Wu's Experimental Animal Trade Co., Ltd., Fuzhou city, China) and sterile water; (iii) high-fat diet plus non-fermented black tea beverage group (HFD + NF), fed with a high-fat diet and a non-fermented black tea beverage; (iv) high-fat diet plus fermented black tea beverage group (HFD + F), fed a high-fat diet and sterilized black tea beverage after fermentation mentioned above; and (v) high-fat diet plus simvastatin group (HFD+Simv), fed with a high-fat diet and sterile water containing 10 mg/L simvastatin (Li, et al., 2022)

2.2 Body weight measurement and samples collection

The body weight of mice in each group was measured using digital electronic scales every 3 days throughout the 8 weeks experimental period. At the end of the experiment, mice were fasted for 12 h, anesthetized with diethyl ether, and then euthanized. Samples of blood, feces, cecal contents, liver tissue, and epididymal adipose tissue were collected for subsequent analysis. Blood samples were

centrifuged at 1500 g for 15 min at 4 ℃ to obtain serum for biochemical analysis. Epididymal adipose tissue was weighed, while fresh feces were collected, treated with liquid nitrogen, and stored at -80 ℃ for preservation. Livers were harvested, imaged, and fixed in 4% paraformaldehyde for subsequent histopathological analysis.

2.3 Biochemical Analysis of Serum

The serum biochemical indicators, including total cholesterol (TC), triglycerides (TG), high-density lipoprotein cholesterol (HDL-c), and low-density lipoprotein cholesterol (LDL-c), were quantified using a biochemical analyzer manufactured by Servicebio Technology Co., Ltd. in Wuhan, China.

2.4 Histopathologic Evaluation of Mice Liver Tissue

Hematoxylin and eosin (H&E) staining as well as oil red O staining were conducted to assess the hepatic histopathology of mice. In brief, the liver tissues were dehydrated using a series of alcohol gradients and subsequently embedded in paraffin wax blocks. Afterwards, 5 μm thick sections were obtained through dewaxing, hydration, staining, dehydration and sealing processes. The fixed hepatic tissues were subsequently immersed in a 30% sucrose solution overnight, followed by embedding in OCT and slicing into sections of 6 to 8 μm thickness using a freezing microtome. The standard staining protocols were employed, including washing, H&E or oil red O staining, differentiation, and sealing. Finally, both H&E and oil red O stained sections were examined using a Nikon Intensilight C-HGF1 microscope (Nikon, Japan).

2.5 Quantitative Real-Time PCR (RT-qPCR)

The Quantitative Real-Time PCR analysis was couducted following a previously described method [22], the detailed description is provided in the supplementary materials.

2.6 The Western blot

The protein expression levels of TLR4 and ALDH2 were examined using western blot analysis, and the detailed description is provided in the supplementary materials.

2.7 Metabolomic Analysis using UPLC-QTOF/MS

The analysis of hepatic lipid metabolome in mice was conducted using the previously described methodology[23], the detailed description is provided in the supplementary materials.

2.8 High-Throughput Sequencing Analysis of Gut Microbiome

The fecal samples of mice from different groups were collected and placed in a sterile sampling bag, followed by being rapidly frozen using liquid nitrogen. Subsequently, the total microbial DNAs was extracted using GenElute™ soil DNA separation kit (Sigma-Aldrich Co. LLC, USA). The 16S rRNA gene (V3 and V4 hypervariable regions) of the bacterial colony was amplified using a special primer (forward primer 5’-ACTCCTACGGGAGGCAGCAG-3’and reverse primer 5’-GGACTACHVGGGTWTCTAAT-3’). The PCR was performed using 15 μL of Phusion® High-Fidelity PCR Master Mix, 2 μM of forward and reverse

primers, and approximately 10 ng of template DNA. Additionally, the thermal cycling protocol is outlined as follows: one cycle of cDNA synthesis at 37°C for 15 min and one cycle of initial PCR activation at 95°C for 30 s, followed by 40 cycles of denaturation at 95°C for 5 s, annealing at 55°C for 31 s, and extension at 95°C for 5 s, followed by one cycle of final extension at 72°C for 30 s. The PCR products were mixed with an equal volume of 1× loading buffer, subjected to electrophoresis on a 2% agarose gel for detection, and then purified using the Qiagen Gel Extraction Kit (Qiagen, Germany) in equidensity ratios. Furthermore, the sequencing libraries were prepared using the TruSeq® DNA PCR-Free Sample Preparation Kit (Illumina, USA) according to the manufacturer's instructions and indexed. The library was sequenced using a paired-end (2×300) approach on an Illumina MiSeq PE300 platform by Beijing Novogene Technology Co., Ltd (Beijing, China), following standard protocols. The quality-filtered sequences were clustered into operational taxonomic units (OTUs) with 97% similarity threshold using Uparse software (Uparse v7.0.1001, http://www.drive5.com/uparse/). Additionally, the species annotation analysis was performed using the Mothur method and the SSUrRNA from the SILVA132 database (http://www.arb-silva.de/). Moreover, α and β diversity analysis was conducted using the Qiime software (Version 1.9.1).

2.9 Examination of short-chain fatty acid

Fresh murine fecal samples were collected and analyzed for short-chain fatty acids (SCFAs) content using a validated, previously published method[24].

2.10 Statistical Analysis

All data are presented as the mean ± standard deviation. The statistical significance analysis of the test results is carried out by one-way analysis of variance using Origin 2018. The significance levels were set at $P < 0.05$ and $P < 0.01$, indicating statistical and extremely significant differences, respectively.

3. Results

3.1 Changes in body weight and epididymal fat weight of mice

Body weight and epididymal fat mass are core indicators for evaluating high-fat diet-induced adipose tissue accumulation in mouse models. In this study, high-fat diet intervention is sustained for 8 weeks, and four distinct experimental treatments are implemented simultaneously: purified water (negative control), unfermented black tea beverage, fermented black tea beverage (FBTB), and simvastatin solution (positive control) (Fig. 2A). Compared with the HFD group, the body weight and epididymal fat weight of mice in the HFD + NF and HFD+Simv groups exhibit a slight reduction. In contrast, the corresponding indicators of mice in the HFD + F group decrease significantly when compare with those in the HFD, HFD + NF and HFD+Simv groups (Fig. 2B, C). It was found that the administration of FBTB alleviates the accumulation of adipose tissue in mice.

3.2 The impact of FBTB on serum lipid levels

Serum lipid levels are recognized as pivotal indicators that accurately reflect lipid metabolic homeostasis. Compared with the normal diet (NFD) group, the serum levels of total cholesterol (TC), triglycerides (TG) and low-density lipoprotein cholesterol (LDL-c) in mice of the high-fat diet (HFD) group are significantly elevated ($P < 0.05$), while the level of high-density lipoprotein cholesterol (HDL-c) demonstrates a moderate reduction. However, the HFD + F group exhibits significantly reduced serum levels of TC, TG and LDL-c, alongside a notable increase in HDL-c ($P < 0.05$). Moreover, only a reduction in serum TG levels is found in HFD + NF group, whereas both decreased TG levels and elevated low-density lipoprotein cholesterol (LDL-c) levels are detected in the HFD+Simv groups (Fig. 3A-3D).

Furthermore, the morphological alterations in the liver of mice were observed. As shown in Fig. 3E, liver tissues of mice in the ND group exhibit normal coloration, morphology, and size. In contrast, livers from the HFD group display the characteristic features of NAFL, including hepatic hypertrophy, a grayish-white to earthy-yellow appearance, and numerous fat vacuoles induced by adipose tissue accumulation. The abnormal pathological phenotypes in the livers of mice are significantly alleviated in the HFD + F group, while moderate ameliorative effects are observed in the HFD + NF and HFD+Simv groups. Furthermore, Oil Red O staining and hematoxylin-eosin staining were performed to confirm the morphological alterations of hepatic tissues at the microscopic level. As shown in Fig. 3F-3G, adipocytes and lipid droplets are widely distributed throughout the liver tissues of mice in the HFD group. In contrast, a significant reduction in adipocyte content is observed in the HFD + F group, while a moderate decrease is detected in both the HFD + NF and HFD+Simv groups. These findings indicate that supplementation with FBTB can effectively alleviate NAFL symptoms in mice.

3.3 Effects of FBTB on Genes and proteins Expression Related to Hepatic Lipid Metabolism

As shown in Fig. 4, in the HFD group, the gene expression levels of Hepatic Lipase (*HL*), Acetyl-coa acetyltransferase 1 (*Acat*1), and Acetyl-CoA Carboxylase Alpha (*Acaca*) are significantly up-regulated, whlie the expression levels of Carnitine palmitoyltransferase 1A (*Cpt*1a) and lecithin-cholesterol acyltransferase (*Lcat*) are down-regulated. Moreover, the protein expression level of Toll-like receptor 4 (TLR4) is down-regulated, and the expression of aldehyde dehydrogenase 2 (ALDH2) is significantly up-regulated. Compared with the HFD group, the gene expression levels of *HL*, *Acat*1, and *Acaca* are significantly elevated in the HFD + F group. In contrast, the expression levels of *Cpt1a* and Lcat are increased. Furthermore, the protein expression level of TLR4 is up-regulated, and ALDH2 expression is significantly down-regulated. It was indicated that FBTB intervention promotes the restoration of the expression levels of these genes and proteins in high-fat diet-induced NAFL mice. The expression variation trends of the aforementioned genes and proteins in the HFD+Simv group are consistent with those observed in the HFD + F group.

3.4 Effects of FBTB on Liver Lipid Metabolites

The hepatic lipid metabolic profiles of the mice were examined via ultra performance liquid chromatography-quadrupole time of flight-mass spectrometry (UPLC-QTOF-MS), operated in both positive and negative ionic modes. As shown in Fig. 5(A-D) and 6(A-D), based on the PCA analysis in both positive and negative ionization modes, significant differences are demonstrated in the hepatic lipid metabolic profiles among mice from the NFD, HFD, and HFD + F groups. Additionally, as shown in Fig. 5E, a total of 176 lipid metabolites in the positive ionization mode are identified across the three groups. Among them, 71 lipid compounds, including PC(20:1/22:5), DAG(16:0/22:5), LPE 20:2, LPC 16:1, LPE 20:1, CL(18:0–18:3–20:4–20:4), LPC 20:1, (3E,5E,7E,9E)-3,5,7,9,11-Dodecapentaenoic acid, TAG(18:1–19:1–20:3), PC(22:0/22:6), PC(17:2/17:2), PC(19:0/22:5), PC(22:3/16:4), PE(16:1/22:6), PG(16:0/18:3), DAG(22:1/20:4), cerebroside, Chamazulene, Lycopene, Hydroxyprogesterone, p-cymene, gualazulene and Retinol palmitate, are detected in both the HFD + F group and NFD group but are absent in the HFD group. The findings suggest that the implementation of FBTB intervention can restore the normal anabolism of the aforementioned lipids in the liver of NAFL mice. Additionally, 30 lipids, such as SM(d16:0/22:0), Triolein, BMP(18:1/22:6), SM(d28:1/12:1), ACar 21:1, Menaquinone 9, PC(22:4e/25:0), certonardosterol, PC(10:0/13:1), PC(22:6e/16:4), PS(18:1/18:2), PC(20:4e/22:5), 1,2-dioleoyl-sn-glycero-3-phosphoserine, ACar 19:1, ACar 21:0, ACar 21:2, ACar 22:1, (5Z,8Z)-tetradecadienoylcarnitine, O-behenoylcarnitine, DAG(18:1/20:3), PC(18:0/22:5), PC(11:0/11:0), PE(18:5e/22:0), TAG(18:2–18:2–22:6), PC(14:1e/24:4), PE(18:5e/22:0), Lexacalcitol, PC(18:0/20:5), PC(18:3/24:4), are exclusively identified in the HFD group. It is suggested that FBTB supplementation can effectively enhance the levels of the aforementioned lipids in the liver.

Besides, a total of 68 lipids are identified in the negative ionization mode. In comparison to the NFD group, the HFD group exhibits the presence of various lipid compounds, including TxB2, stearic acid, SM (d14:1/24:0), OxPC (18:0–20:4 + 3O(2Cyc)), OxPC (18:0–20:3 + 3O(1Cyc)), FAHFA (16:0/2:0), ascr26, Cer-NP (t18:0/20:0), PI (17:0/20:4), PE (4:0/18:0), tetranor-prostaglandin, PG (18 : 1 /22 : 4) and PC (18 : 1e / 18 : 1). Conversely, the lipids such as PS(18:2/20:4), PG(20:3/22:4), PC(16:0e/24:4), PE(16:1/16:1), SM(d14:3/27:0), PE(18:3/22:6), CL(18:1–20:3–18:2–22:6), LPI 22:4, PE(16:1/18:3), PG(14:0/18:2), Docosahexaenoyl PAF C-16, PC(16:1/20:5), SM(d20:2/21:0), SM(d14:3/29:0), Quillaic Acid, 1-Oleoyl-2-hydroxy-sn-glycero-3-PE, LPG 16:0, 1-[(9Z)-hexadecenoyl]-sn-glycero-3-phosphocholine, LPI 20:1, PC(16:0e/22:6), CL(16:1–18:2–18:2–18:2), CL(16:1–18:2–18:2–22:6), PC(16:1/22:6) and PE(19:0/20:4) are absent.

However, in the HFD + F group, the absence of the lipid compounds identified in HFD group, including 1-Oleoyl-2-hydroxy-sn-glycero-3-PE, 1-[(9Z)-hexadecenoyl]-sn-glycero-3-phosphocholine, LPI 20:1, PC(16:0e/22:6), CL(16:1–18:2–18:2–18:2), CL(16:1–18:2–18:2–22:6), PC(16:1/22:6) and PE(19:0/20:4) are observed, and additional lipids such as CL(18:1–22:6–18:2–18:6), PE(18:0/20:1) and LPI 20:3 are observed. Moreover, the lipids involving PS(18:2/20:4), PG(20:3/22:4), PC(16:0e/24:4), PE(16:1/16:1), SM(d14:3/27:0), PE(18:3/22:6), CL(18:1–20:3–18:2–22:6), LPI 22:4, PE(16:1/18:3), PG(14:0/18:2),

Docosahexaenoyl PAF C-16, PC(16:1/20:5), SM(d20:2/21:0), SM(d14:3/29:0) and Quillaic Acid fail to be found (Fig. 6E).

Furthermore, the metabolic pathway enrichment analysis of differentially produced hepatic metabolites is conducted using MetaboAnalyst 4.0 based on KEGG to visualize the alterations of metabolic pathways in response to FBTB intervention. The results of positive-ion mode metabolic pathway enrichment analysis indicate that FBTB intervention demonstrates significant affects on the Sphingolipid metabolism, Retinol metabolism, Glycerophospholipid metabolism, Steroid biosynthesis, steroid hormone biosynthesis, alpha-linolenic acid metabolism, Taurine and hypotaurine metabolism and Glycosylphosphatidylinositol (GP)-anchor biosynthesis (Fig. 5F). In negative-ion mode, FBTB intervention induces distinct alterations in lipid metabolic pathways compared to HFD-fed mice, primarily including Arachidonic acid metabolism, Linoleic acid metabolism, Biosynthesis of unsaturated fatty acid, Glycerophospholipid metabolism, Primary bile acid biosynthesis, alpha-linolenic acid biosynthesis, Glycosylphosphatidy linositol (GPI)-anchor biosynthesis, Sphingolipid metabolism, as well as Pentose and glucuronate inter-conversions (Fig. 6F).

3.5 The effect of FBTB on the mice gut microbiota

To investigate the impact of FBTB intervention on the gut microbiota of high-fat diet-fed mice, high-throughput sequencing was conducted. As shown in Figure S1, the rarefaction curve and rank abundance curve are employed to illustrate the diversity of samples within a specific group. It can be observed that the rarefaction curve for mice intestinal flora initially rises before reaching a plateau, while the rank abundance curve exhibits a gradual slope with relatively uniform species distribution. These observations confirm that the sample size is sufficient, providing robust analytical support. Based on the OTU clustering results and research requirements, the microbial flora sequencing data of all samples were standardized, and an OTU-based petal plot was constructed. The NFD group harbors 650 microbial community OTUs, indicating a diverse species composition of the intestinal flora. The HFD group has 88 unique intestinal flora OTUs. By contrast, the other three intervention groups—HFD + F, HFD+Simv, and HFD + NF—have 283, 191, and 114 unique OTUs, respectively (Figure S2). The results indicate that FBTB intervention can significantly increase the species richness of intestinal microbiota in high-fat diet-fed mice.

The composition of the intestinal microbial community at the phylum level in mice from the HFD + F group differs significantly from that of the other groups (Figure S3). Based on the data presented in Fig. 7A, *Bacteroidota* (53.7%) and *Firmicutes* (24.3%) are the dominant phyla in the colon of mice in the normal-fat diet (NFD) group. Furthermore, Unidentified Bacteria (5.7%), *Proteobacteria* (5.8%), and *Verrucomicrobiota* (3.8%) are also detected in this cohort. In contrast, the relative abundances of *Bacteroidota* and *Verrucomicrobiota* in the HFD group are significantly decreased to 24.2% and 11.5%, respectively, while the relative abundances of *Firmicutes*, unclassified Bacteria and *Proteobacteria* increased to 36.8%, 16.6%, and 12.8%. Compared with the HFD group, the relative abundances of *Bacteroidota*, *Proteobacteria* and *Campylobacterota* in the HFD + F group are 2.8-fold, 2.7-fold and 5.8-fold

of that in the HFD group, representing a 1.8-fold, 1.7-fold and 4.8-fold increase relative to the HFD group, respectively. Conversely, the relative abundances of *Firmicutes* and *Verrucomicrobota* decrease by 1.7-fold and 33.2-fold. Compared with the HFD group, the HFD + NF group exhibits a 1.2-fold increase in the relative abundance of *Bacteroidota* and a 1.5-fold increase in that of *Firmicutes*; Meanwhile, the relative abundances of unidentified bacteria, *Proteobacteria* and *Verrucomicrobota* decreased by 1.4-fold, 1.9-fold and 10.4-fold, respectively. Furthermore, compared with the HFD group, the relative abundances of *Bacteroidota* and *Proteobacteria* increased by 1.6-fold and 3.3-fold, respectively; In contrast, the relative abundances of *Firmicutes*, unclassified bacteria, and *Verrucomicrobiota* decrease by 1.5-fold, 2.4-fold, and 1.6-fold.

As shown in Fig. 7B, at the Genera level, the colonic microbiota of mice in the NFD group are dominated by *lactobacillus, Akkermansia, Lachnospiraceae, Odoribacter, Alistipes* and *Bacteroides*. However, in the HFD group, the relative abundance of *Lactobacillus*, *Akkermansia* and *Bcteroides* decrease by 1.8-fold, 24.2-fold and 1.7-fold respectively; While the relative abundances of *Lachnospiraceae*, *Odoribacter*, *Alistipes*, *Helicobacter* increase by 1.7-fold, 3.3-fold, 8.3-fold and 3.3-fold. Moreover, compared to the HFD group, there is a significant increase in the relative abundances of *Lactobacillus* (117.5-fold), *Akkermansia* (5.6-fold) and *Dubosiella* (17.6); Nevertheless, a marked decrease is found in the relative abundances of *Alistipes* (22-fold) *Bacteroides* (1.6-fold), *Helicobacter* (2.1-fold) and *Alloprevotella* (1.5-fold) in the HFD + F group. Compared with the HFD group, the HFD + NF group exhibits a significant decrease in the relative abundances of *Lactobacillus* (2.8-fold), *Akkermansia* (43.3-fold), *Bacteroides* (1.8-fold) and *Alloprevotella* (1.8-fold); By contrast, the abundances of *Lachnospiraceae* (1.2-fold), *Odoribacter* (13.8-fold), *Alistipes* (6.3-fold) and *Helicobacter* also show a marked reduction. Furthermore, compared with the HFD group, mice in the HFD+Simv group exhibit a 2.4-fold increase in the relative abundance of *Lactobacillus*, a 31.2-fold increase in the relative abundance of *Akkermansia*, a 1.3-fold decrease in the relative abundance of *Bacteroides*, a 5.2-fold increase in the relative abundance of *Alloprevotella*, and a 2.8-fold increase in the relative abundance of *Parasutterella*. In contrast, the relative abundances of *Lachnospiraceae*, *Odoribacter*, *Alistipes*, and *Helicobacter* show significant reductions of 4.1-fold, 9.2-fold, 7.1-fold, and 27.7-fold, respectively.

In comparison to the HFD group, at the Species level, intervention with FBTB significantly elevate the levels of *Akkermansia muciniphila* (39.6-fold) and *Lactobacillus johnsonii* (37.7-fold); Moreover, a noticeable enhancement in levels of *Akkermansia muciniphila* (4.2-fold), *Lactobacillus murinus* (13.5-fold) and *Lactobacillus reuteri* (11.2-fold) are observed in the HFD + F group; Furthermore, a remarkable increase in levels of *Akkermansia muciniphila* (27.2-fold), *Lactobacillus reuteri* (3.3-fold) and *Phascolarctobacterium faecium* (2.2-fold) are found in the HFD+Simv group (Fig. 7C).

3.6 The short-chain fatty acid

As shown in Fig. 8, compared with mice in the normal-fat diet (NFD group, the levels of short-chain fatty acids—including acetic acid, propionic acid, butyric acid, and isobutyric acid—in the feces of mice in the HFD group decrease significantly. Additionally, the concentrations of the aforementioned short-chain

fatty acids in the HFD + F group are elevated to levels comparable to those observed in the NFD control group. In contrast, the concentrations of acetic acid, propionic acid, and butyric acid in the HFD + NF and HFD+Simv groups are lower than those in the HFD + F group.

3.7 The Correlations between gut Microbiota and Metabolites.

Current evidence indicates that targeting the intestinal microbiota has substantial therapeutic potential for non-alcoholic fatty liver disease (NAFL). Accordingly, Spearman correlation analysis was used to generate heatmaps and network graphs visualizing the correlation between key gut microbial phylotypes and hepatic lipid metabolites (as shown in Fig. 9). The findings reveal a positive correlation between *Lactobacillus* abundance and the levels of the following metabolites: PC (17:1/17:2), PC (19:1/22:6), Docosahexaenoyl PAF C-16, LPE 16:1, LPE 17:1, 1-[(9Z)-hexadecenoyl]-sn-glycero-3-phosphocholine, and 1-Oleoyl-2-hydroxy-sn-glycero-3-PE. Additionally, *Akkermansia* demonstrates a positive correlation with TAG (15:2–16:0–20:4), Catacerebroside C, Cer-NS(d18:2/23:0), PC(17:1/17:2), PC(19:1/22;6), Docosahexaenoyl PAF C-16, 1-Stearoyl − 2-docosahexanoyl-sn-glycero-3hposphocholine, DAG (22:21/20:4), LPE16:11, LPE 17:11, l-[(9Z)-hexadecenoyl]-sn-glycero-3-phosphocholine, l-Oleoyl-2-hydroxyglycerol-sn-glycero-3-phospholine and LPC15:0, and is negatively associated with PC(11:0/11:0), PC(18:0/20:5), PS(20:2/20:2) and stearic acid. Moreover, *Dubosiella* exhibits a positive correlation with PC(22:3/16:4), Catacerebroside C, Cer-NS(d18:2/23:0), PC(17:1/17:2), PC(19:1/22:6), Docosahexaenoyl PAF C-16, and LPC15:0. Meanwhile, it also displays a negative correlation with PC(11:0/11:0), PS(20:2/20:2), and Stearic acid. In addition, *Mucispirillum* is positively correlated with PC (11:0/11:0) and PC (18:0/20:5), as well as a negative correlation with TAG (15:2–16:0–20:4) and Catacerebroside C. Furthermore, CHKC1001 is positively correlated with PC (11:0 /11:0) but negatively correlated with PC (15:0/22:6), PC (22:3/16:4), Catacerebroside C, and TAG (17:0–19:1–19:2). *Desulfovibrio* displays a positive correlation with PC (18:0/20:5) and l-stearoyl-2-arachidonoyl-sn-glycero-3-phospho-lD-myo-inositol, while exhibits a negative correlation with TAG (15:2–16:0–20:4), p-cymene and l-palmitoyl-2oleoylsn-glycero-3-(phospho-rac-(l-glycerol)).

4. Discussion

The prevalence of NAFL has increased substantially in recent years, and this trend is primarily attributable to unhealthy dietary patterns, as well as intrinsic and disease-associated factors[25]. Although currently available hypolipidemic drugs demonstrate certain therapeutic effects, they are correlated with adverse reactions including hepatotoxicity and gastrointestinal discomfort[26]. Therefore, the development of safe and effective strategies for NAFL intervention is of paramount importance.

LAB as one of the predominant probiotic groups, have demonstrated promising preclinical efficacy in ameliorating obesity, NAFL, and insulin resistance[27], and are regarded as a non-invasive, high-potential therapeutic modality for obesity and its related metabolic disorders. For instance, administration of

Bifidobacterium adolescentis and *Lactobacillus rhamnosus* LGG alleviates NAFL in high-fat high-cholesterol diet-induced mice via regulating distinct gut microbiota-dependent pathways. These mechanisms include increasing the concentration of short-chain fatty acids (SCFAs) in the intestines of NAFL mice, regulating energy and lipid metabolism, and attenuating hepatic inflammation[16]. Additionally, *Lactobacillus sakei* MJM60958 effectively mitigates NAFL in mice by modulating lipid metabolism, inflammatory response, and the composition of gut microbiota [28]. Moreover, *Lactiplantibacillus plantarum* DSM20174 alleviates the progression of NAFL through regulation of gut microbiota, improvement of metabolic risk factors, and attenuation of adipose inflammation [14].

Beyond viable cells of LAB strains, LAB-fermented foods also exert similar ameliorative effects on NAFL symptoms. For example, supplementation with *L. plantarum*-fermented black barley effectively alleviates NAFL in high-fat diet-fed rats, primarily through reversing high-fat diet-induced gut microbiota dysbiosis[29]. Milk fermented with *Lactobacillus rhamnosus* alleviates hepatic inflammation, improves tissue oxygenation, and attenuates hepatocyte injury in NAFL rats via the modulation of serum lipid metabolism, amino acid metabolic pathways and associated downstream metabolites[30]. In the present study, following a 2-month intervention with *L. plantarum*-fermented black tea (FBTB), NAFL mice demonstrate significant reductions in body weight, epididymal adipose tissue mass, and hepatic fat accumulation. Furthermore, serum levels of total cholesterol (TC), triglycerides (TG), and low-density lipoprotein cholesterol (LDL-c) decrease significantly, while high-density lipoprotein cholesterol (HDL-c) levels are increased. Collectively, these findings suggest that the functional components in black tea (e.g., tea polyphenols, caffeine), cellular components of *L. plantarum* RLL68, its metabolites (including γ-aminobutyric acid (GABA) and organic acids)[20], as well as SCFAs in FBTB, may contribute to the therapeutic efficacy of FBTB against NAFL.

Following fermentation with *L. plantarum*, eight organic acids were identified in FBTB, including lactic acid, malic acid, acetic acid, citric acid, tartaric acid, formic acid, succinic acid, and propionic acid (as shown in Table S1). Notably, dietary supplements containing acetic acid and propionic acid have been demonstrated to effectively reduce blood glucose, cholesterol, and lipid levels in healthy volunteers[31]. Moreover, addition of acetic acid and propionic acid to a high-fat diet can significantly decrease the TG and TC levels, while also improving glucose homeostasis[32]. The production of acetic acid and propionic acid is closely associated with the abundance of *Bacteroidetes*, which simultaneously contribute to improving the intestinal microecology and increasing the abundance of beneficial bacteria[33].

In addition to organic acids, tea polyphenols, another major functional component of FBTB, have been shown to modulate gut microbiota composition by promoting the proliferation of beneficial bacteria such as *Bacteroides*, *Faecalibacterium*, *Parabacteroides*, and *Akkermansia*, thereby enhancing intestinal barrier function and overall gut health[34]. In this study, NAFL mice received FBTB intervention exhibit a significant increase in the relative abundances of *Lactobacillus* and *Akkermansia*. Accumulating evidence has demonstrated that interventions targeting the enrichment of *Akkermansia muciniphila* effectively ameliorate metabolic traits, including insulin resistance and hepatic steatosis, in patients with obesity

and NAFL[35]. Additionally, *A. muciniphila* treatment enhances mitochondrial oxidation and bile acid metabolism in the gut-liver axis, mitigates oxidative stress-induced intestinal epithelial cell apoptosis, and reshapes gut microbiota composition[36], which may contribute to the alleviation of NAFL pathology. Moreover, supplementation of *Lactobacillus* strains, including *L. acidophilus*, *L. fermentum*, *L. plantarum*, *L. paracasei*, *L. rhamnosus*, and *L. johnsonii*, has been reported to exert beneficial effects on the progression of nonalcoholic steatosis by reducing systemic cholesterol levels and regulating lipid metabolism[37–41]. Collectively, these findings, in conjunction with the results obtained in the present study, support the conclusion that FBTB fermented with *L. plantarum* integrates the bioactive effects of organic acids (e.g., acetic acid and propionic acid), tea polyphenols and probiotic metabolites, thereby demonstrating promising potential for alleviating or preventing NAFL.

As the central hub for systemic lipid metabolism, the liver initiates NAFL development when hepatic steatosis occurs, which is defined as the aberrant accumulation of triacylglycerols (TAGs) within hepatocytes[42]. Dysregulated lipid droplet dynamics, impaired lipoprotein secretion, and disrupted bile acid homeostasis collectively promote excessive lipid deposition; Meanwhile, aberrations in phospholipid levels and composition further perturb hepatic neutral lipid metabolism, promoting the progression from NAFL to non-alcoholic steatohepatitis (NASH)[43]. To investigate the regulatory effects of FBTB on hepatic lipid metabolism, we performed lipid profile analysis on liver tissues from NAFLmice using UPLC-QTOF-MS in both positive and negative ionization modes. FBTB intervention significantly restores the hepatic levels of unsaturated lipids and functional phospholipids, including phosphatidylcholines (PCs: 20:1/22:5, 22:0/22:6, 17:2/17:2, 19:0/22:5, 22:3/16:4), phosphatidylethanolamine (PE: 16:1/22:6), phosphatidylglycerol (PG: 16:0/18:3), diacylglycerol (DAG: 16:0/22:5), TAG (18:1–19:1–20:3), cerebroside, lycopene, and (3E,5E,7E,9E)-3,5,7,9,11-dodecapentaenoic acid. These bioactive lipids have been documented to exert protective effects against non-alcoholic fatty liver (NAFL); For example, polyene phosphatidylcholine, a formulation rich in phosphatidylcholine (PC), is clinically applied in the treatment of NAFL[44]. The cerebroside can attenuate hepatic steatosis by inhibiting hepatic lipogenic gene expression and enhancing hepatic TAG secretion[45]. Besides, lycopene prevents steatohepatitis and inhibits NASH-associated early hepatocarcinogenesis in high-fat diet-fed rats[46]. Conversely, FBTB intervention reduced hepatic levels of pro-steatotic saturated lipids, including thromboxane B2 (TxB2), stearic acid, fatty acid ester of hydroxy fatty acid (FAHFA: 16:0/2:0), non-hydroxy ceramide (Cer-NP: t18:0/20:0), PE (4:0/18:0), and tetranor-prostaglandin. Saturated fats are well-documented to promote NAFL pathogenesis[47], and elevated serum TxB2 levels are linked to obesity[48], highlighting the functional significance of FBTB-mediated suppression of these detrimental lipids.

A core component of the mechanistic framework is the crosstalk between gut microbiota remodeled by FBTB and hepatic lipid metabolism. FBTB-induced elevations in the relative abundances of *Lactobacillus* and *Akkermansia* show strong correlations with hepatic lipid profiles: these beneficial microbes are positively associated with hepato-protective lipids (e.g., TAG (15:2–16:0–20:4), catacerebroside C, Cer-NS (d18:2/23:0), PCs (17:1/17:2, 19:1/22:6), docosahexaenoyl PAF C-16, 1-stearoyl-2-docosahexanoyl-sn-glycero-3-phosphocholine, DAG (22:2/20:4), lysophosphatidylethanolamines (LPEs: 16:1, 17:1), 1-

[(9Z)-hexadecenoyl]-sn-glycero-3-phosphocholine, 1-oleoyl-2-hydroxyglycerol-sn-glycero-3-phosphocholine, 1-oleoyl-2-hydroxy-sn-glycero-3-PE) and negatively correlated with pro-steatotic lipids (e.g., PC(11:0/11:0), PC(18:0/20:5), stearic acid). This microbiota-lipid interaction is hypothesized to occur via multiple pathways: (1) FBTB supplementation promotes the production of short-chain fatty acids (SCFAs, e.g., acetic acid and propionic acid), which function as signaling molecules to modulate hepatic fat deposition and metabolic disorders; (2) increased abundance of Akkermansia and Lactobacillus strains may enhance intestinal barrier function, alleviating hepatic inflammation and lipid dysregulation induced by endotoxemia; and (3) both genera regulate bile acid metabolism along the gut-liver axis, further modulating hepatic lipid absorption and metabolism.

Furthermore, FBTB intervention reprograms the expression of key genes and proteins governing hepatic lipid homeostasis, which synergizes with microbiota-lipid crosstalk to restore metabolic balance of lipids. At the transcriptional level, FBTB intervention down-regulates the expression of *Acaca* (Acetyl-CoA carboxylase α, a rate-limiting enzyme in fatty acid synthesis) and Acat1 (Acyl-CoA cholesterol acyltransferase 1, which promotes cholesterol esterification), which is consistent with the reduced saturated lipid levels. Additionally, it up-regulates Cpt1a (Carnitine palmitoyltransferase 1a, the rate-limiting enzyme in mitochondrial fatty acid β-oxidation), HL (Hepatic lipase, which hydrolyzes TAGs in lipoproteins), thereby enhancing hepatic lipid decomposition and clearance, and Lcat (Lecithin-cholesterol acyltransferase), which facilitates HDL-mediated cholesterol efflux, thus improving reverse cholesterol transport and reducing hepatic cholesterol accumulation.

At the protein level, FBTB was found to regulate the protein expression of Toll-like Receptor 4 (TLR4) and Aldehyde Dehydrogenase 2 (ALDH2), both of which are key molecules closely associated with lipid metabolism and the pathogenesis of NAFL. As a core mediator of endotoxin-induced inflammation, TLR4 promotes the development of hepatic steatosis by activating pro-inflammatory signaling pathways that disrupt lipid homeostasis[49]. FBTB-mediated downregulation of TLR4 (likely achieved via improvement of intestinal barrier function) alleviates hepatic inflammation and reduces lipid accumulation. ALDH2, which participates in fatty acid oxidation and the detoxification of lipid-derived aldehydes, exerts a protective effect against NAFL by promoting lipid catabolism and attenuating oxidative stress[50]. FBTB intervention-induced upregulation of ALDH2 further enhances hepatic lipid clearance.

5. Conclusion

In the present study, our findings demonstrate that FBTB intervention ameliorates NAFL in mice primarily via remodeling gut microbiota and restoring hepatic lipid homeostasis. FBTB upregulates hepatic levels of cytoprotective unsaturated lipids and functional phospholipids, while downregulating the accumulation of pro-steatotic saturated lipids. Meanwhile, FBTB modulates gut microbiota by significantly enhancing the relative abundances of beneficial bacteria. These beneficial bacteria are positively correlated with hepatoprotective unsaturated lipids, and negatively correlated with steatosis-promoting saturated lipids and esters. These correlations between microbes and lipids, in conjunction

with the transcriptional and translational reprogramming of key lipid metabolism-related genes and proteins identified in this study, collectively highlight the multiple pathways through which FBTB alleviates NAFL. These findings not only corroborate that FBTB is a promising nutraceutical intervention for NAFL, but also promote the development of LAB-fermented foods with ameliorative or preventive efficacy against NAFL and its associated metabolic disorders.

Declarations

Funding Declaration

This study was supported by Fujian Provincial Natural Science Foundation (No. 2024J01360) and the Open Project Program of the Key Laboratory of Brewing Molecular Engineering of China Light Industry.

Author contributions

Jinzhi Han, Yifeng Liu conceived and designed research. Ruili Li, Anxin Sun, Xinghu Lu conducted experiments. Ruili, Li, Xinghu Lu, Yifei Lu and Chong Xu analyzed data. Ruili Li and Chong Xu wrote the manuscript. Yifeng Liu, Yifei Lu, Chong Xu provided the modification of this manuscript. All authors read and approved the manuscript, and all authors declare that they have no conflict of interest.

Competing Interest declaration

All authors read and approved the manuscript, and all authors declare that they have no conflict of interest.

Data Availability declaration

The data that support the findings of this study are available from the corresponding author upon reasonable request.

References

1. Faruk O, Ahmed KU, Ishrat N, Mrittika SA, Alam S, Hasan M, Tanjum FA, Mohammad N, Mahmud A, Amin MN (2026) Liver cirrhosis: epidemiology, risk factors, potential complications, and possible treatment strategies. Gastroenterology & Endoscopy
2. Wei C, Cheng S, Zhang Y, Zhao Y, Wei H, Wang F, Wang J-H, Jiang D, Wang Z (2026) A liver-targeting fluorescent nano-drug for theranostics in non-alcoholic fatty liver disease, Biomaterials 124182
3. Betlejewska J, Hubska J, Roszkowska Z, Maciejczyk A, Bachurska D, Domański J, Miarka M, Raszeja-Wyszomirska J, Bobrowicz M, Ambroziak U (2025) Endocrine disorders and metabolic dysfunction-associated steatotic liver disease: a narrative review. Biomedicines 13(10):2500
4. Rotman Y, Sanyal AJ (2017) Current and upcoming pharmacotherapy for non-alcoholic fatty liver disease. Gut 66(1):180–190

5. Op CJ, ‘t Hoog LA, de Jong J, Sijm M, Smits SF, Mulder E, Boerrigter (2026) Etoposide dosing challenges in a testicular cancer patient with hepatic impairment and drug-drug interactions–a case report. Cancer Chemother Pharmacol 96(1):18
6. Yu C, Guo X, Cui X, Su G, Wang H (2024) Functional food chemical ingredient strategies for non-alcoholic fatty liver disease (NAFLD) and hepatic fibrosis: chemical properties, health benefits, action, and application. Curr Nutr Rep 13(1):1–14
7. Ren J, Jiang T, Wei X, Bian T, Xu M, Zhao Y, Zheng Y, Li X (2026) Unravelling the Mechanisms of Tea Against NAFLD: An Integration of Bibliometrics, Network Pharmacology, and the Gut-Liver Axis. Diab/Metab Res Rev 42(1):e70118
8. Raj T, Chandrasekhar K, Kumar AN, Kim S-H (2021) Recent biotechnological trends in lactic acid bacterial fermentation for food processing industries. Syst Microbiol Biomanufacturing 1–27
9. Özcelik S, Kuley E, Özogul F (2016) Formation of lactic, acetic, succinic, propionic, formic and butyric acid by lactic acid bacteria. LWT 73:536–542
10. Zhou Yang ZY, Cui YanHua CY, Qu QX, XiaoJun (2019) Exopolysaccharides of lactic acid bacteria: structure, bioactivity and associations: a review
11. Marulo S, De Caro S, Nitride C, Di Renzo T, Di Stasio L, Ferranti P, Reale A, Mamone G (2024) Bioactive peptides released by lactic acid bacteria fermented pistachio beverages. Food Bioscience 59:103988
12. Wei B, Peng Z, Xiao M, Huang T, Yang S, Liu K, Wu M, Zheng W, Xie M, Xiong T (2023) Modulation of the microbiome–fat–liver axis by lactic acid bacteria: A potential alleviated role in high-fat-diet-induced obese mice. J Agric Food Chem 71(27):10361–10374
13. Nagashimada M, Honda M (2021) Effect of microbiome on non-alcoholic fatty liver disease and the role of probiotics, prebiotics, and biogenics. Int J Mol Sci 22(15):8008
14. Riezu-Boj JI, Barajas M, Pérez-Sánchez T, Pajares MJ, Araña M, Milagro FI, Urtasun R (2022) Lactiplantibacillus plantarum DSM20174 attenuates the progression of non-alcoholic fatty liver disease by modulating gut microbiota, improving metabolic risk factors, and attenuating adipose inflammation. Nutrients 14(24):5212
15. Kang Y, Kang X, Yang H, Liu H, Yang X, Liu Q, Tian H, Xue Y, Ren P, Kuang X (2022) Lactobacillus acidophilus ameliorates obesity in mice through modulation of gut microbiota dysbiosis and intestinal permeability. Pharmacol Res 175:106020
16. Wang G, Jiao T, Xu Y, Li D, Si Q, Hao J, Zhao J, Zhang H, Chen W (2020) Bifidobacterium adolescentis and Lactobacillus rhamnosus alleviate non-alcoholic fatty liver disease induced by a high-fat, high-cholesterol diet through modulation of different gut microbiota-dependent pathways. Food Funct 11(7):6115–6127
17. Shen S, Liu Y, Wang N, Huang Z, Deng G (2025) The role of microbiota in nonalcoholic fatty liver disease: mechanism of action and treatment strategy. Front Microbiol 16:1621583
18. Anis MA, Shahid Y, Majeed AA, Abid S (2025) Microbiome and gut-liver interactions: From mechanisms to therapies. World J Gastroenterol 31(40):111409

19. Pabst O, Hornef MW, Schaap FG, Cerovic V, Clavel T, Bruns T (2023) Gut–liver axis: barriers and functional circuits. Nat Reviews Gastroenterol Hepatol 20(7):447–461
20. Li R, Luo W, Liu Y, Chen C, Chen S, Yang J, Wu P, Lv X, Liu Z, Ni L (2022) The investigation on the characteristic metabolites of Lactobacillus plantarum RLL68 during fermentation of beverage from by-products of black tea manufacture. Curr Res Food Sci 5:1320–1329
21. Huang Z-R, Chen M, Guo W-L, Li T-T, Liu B, Bai W-D, Ai L-Z, Rao P-F, Ni L, Lv X-C (2020) Monascus purpureus-fermented common buckwheat protects against dyslipidemia and non-alcoholic fatty liver disease through the regulation of liver metabolome and intestinal microbiome. Food Res Int 136:109511
22. Yang J, Zhang G, Yang X, Peng M, Ge S, Tan S, Wen Z, Wang Y, Wu S, Liang Y (2022) An oral Super probiotics with versatile self-assembly adventitia for enhanced intestinal colonization by autonomous regulating the pathological microenvironment. Chem Eng J 446:137204
23. Chen M, Guo WL, Li QY, Xu J, Lv XC (2020) The protective mechanism of Lactobacillus plantarum FZU3013 against non-alcoholic fatty liver associated with hyperlipidemia in mice fed a high-fat diet. Food Funct 11(6)
24. Zhang Y, Tu S, Ji X, Wu J, Meng J, Gao J, Shao X, Shi S, Wang G, Qiu J (2024) Dubosiella newyorkensis modulates immune tolerance in colitis via the L-lysine-activated AhR-IDO1-Kyn pathway. Nat Commun 15(1):1333
25. Katsiki N, Mikhailidis DP, Mantzoros CS (2016) Non-alcoholic fatty liver disease and dyslipidemia: an update. Metabolism 65(8):1109–1123
26. Frühwald L, Fasching P, Dobrev D, Kaski JC, Borghi C, Wassmann S, Huber K, Semb AG, Agewall S, Drexel H (2025) Management of dyslipidaemia in patients with comorbidities—facing the challenge: Value and limitations of lipid-lowering drugs in liver disease Effects/Interactions of lipid-lowering agents on/with the liver. Eur Heart Journal-Cardiovascular Pharmacotherapy 11(2):164–173
27. Li H, Hu X, Chen H, Chen L, Lin S, Yu C, Hu W (2026) Probiotic intervention in NAFLD: current progress, challenges, and future potential. Food Science and Human Wellness
28. Nguyen HT, Gu M, Werlinger P, Cho J-H, Cheng J, Suh J-W (2022) Lactobacillus sakei MJM60958 as a Potential Probiotic Alleviated Non-Alcoholic Fatty Liver Disease in Mice Fed a High-Fat Diet by Modulating Lipid Metabolism, Inflammation, and Gut Microbiota. Int J Mol Sci 23(21):13436
29. Zhu C, Guan Q, Song C, Zhong L, Ding X, Zeng H, Nie P, Song L (2021) Regulatory effects of Lactobacillus fermented black barley on intestinal microbiota of NAFLD rats. Food Res Int 147:110467
30. Chen D, Liang Y, Liang J, Shen F, Cheng Y, Qu H, Wa Y, Guo C, Gu R, Qian J (2023) Beneficial effects of Lactobacillus rhamnosus hsryfm 1301 fermented milk on rats with nonalcoholic fatty liver disease. J Dairy Sci 106(3):1533–1548
31. Xu J, Qi Y, Wei X, Ding W, Wu H, Liu H, Fang H (2026) Lactobacillus paracasei fermentation enhances the aroma profile and antidiabetic efficacy of goji berry juice. npj Sci Food 10(1):35

32. Liu X, Guan B, Hu Z, Hu X, Liu S, Yang K, Zhou L, Yu L, Yang J, Chen S (2025) Combined traditional Chinese medicine and probiotics (TCMP) alleviates lipid accumulation and improves metabolism in high-fat diet mice via the microbiota-gut-liver axis. Food Res Int 207:116064
33. Ren T, Li D, Sun F, Pan L, Wang A, Li X, Bao Y, Zhang M, Zheng F, Yue H (2025) Indole propionic acid regulates gut immunity: mechanisms of metabolite-driven immunomodulation and barrier integrity. J Microbiol Biotechnol 35:e2503045
34. Wen J-J, Li M-Z, Chen C-H, Hong T, Yang J-R, Huang X-J, Geng F, Hu J-L, Nie S-P (2023) Tea polyphenol and epigallocatechin gallate ameliorate hyperlipidemia via regulating liver metabolism and remodeling gut microbiota. Food Chem 404:134591
35. Dinkov B (2026) Akkermansia muciniphila and GLP-1-based therapies: Bidirectional interactions and implications for type 2 diabetes and MASLD/MASH. Biomedicines 14(6):1235
36. Zhang L, Chen J, Ge S-J, Huang T-Y, Shi X, Chen Y-Y, Lu C-H (2026) Propionic acid secreted by Akkermansia muciniphila alleviates hepatic fibrosis by antioxidant regulation across the gut–liver axis. Life Metabolism 5(1):loaf036
37. Lee NY, Shin MJ, Youn GS, Yoon SJ, Choi YR, Kim HS, Gupta H, Han SH, Kim BK, Lee DY (2021) Lactobacillus attenuates progression of nonalcoholic fatty liver disease by lowering cholesterol and steatosis. Clin Mol Hepatol 27(1):110
38. Ye H, Li Q, Zhang Z, Sun M, Zhao C, Zhang T (2017) Effect of a novel potential probiotic Lactobacillus paracasei Jlus66 isolated from fermented milk on nonalcoholic fatty liver in rats. Food Funct 8(12):4539–4546
39. Zhao Z, Chen L, Zhao Y, Wang C, Duan C, Yang G, Niu C, Li S (2020) Lactobacillus plantarum NA136 ameliorates nonalcoholic fatty liver disease by modulating gut microbiota, improving intestinal barrier integrity, and attenuating inflammation. Appl Microbiol Biotechnol 104:5273–5282
40. Zhang W, Li H, Zhao N, Luo X, Liu S, Bao A, Chen Y, Wang H, Wang J, Wang J (2021) Lactobacillus johnsonii BS15 combined with abdominal massage on intestinal permeability in rats with nonalcoholic fatty liver and cell biofilm repair. Bioengineered 12(1):6354–6363
41. Arellano-García L, Trepiana J, Martínez JA, Portillo MP, Milton-Laskibar I (2023) Beneficial effects of viable and heat-inactivated Lactobacillus rhamnosus GG administration on oxidative stress and inflammation in diet-induced NAFLD in rats. Antioxidants 12(3):717
42. Weiskirchen R, Weiskirchen S, Lonardo A (2026) Lipid droplet dynamics in metabolic regulation. RSC Chem Biology 7(4):517–535
43. Seebacher F, Zeigerer A, Kory N, Krahmer N (2020) Hepatic lipid droplet homeostasis and fatty liver disease, Seminars in cell & developmental biology. Elsevier, pp 72–81
44. Zhang M, Zhang S, Wu H, Xu L, Gao P, Gao Y, Fan W, Song S (2025) Lactobacillus plantarum 1-2-3 inhibits ferroptosis by regulating dysregulated fatty acid metabolism to protect mice from high-fat diet-induced MAFLD. Free Radic Biol Med 238:137–151
45. Cheng C, Wang L, Xie J (2026) Clinical efficacy and mechanism of polyene phosphatidylcholine combined with atorvastatin in treating metabolic associated fatty liver disease. Pak J Pharm Sci

39(2):415

46. Abenavoli L, Procopio AC, Paravati MR, Costa G, Milić N, Alcaro S, Luzza F (2022) Mediterranean diet: the beneficial effects of lycopene in non-alcoholic fatty liver disease. J Clin Med 11(12):3477
47. Tejareh F, Payahoo L, Keshavarz SA (2026) Serum Inflammatory Markers and Dietary Inflammatory Index in Obese Individuals With Fatty Liver Disease: A Case–Control Study, Endocrinology. Diabetes Metab 9(2):e70181
48. Szczuko M, Kwiatkowska L, Szczuko U, Rudak L, Ryterska K, Syrenicz A, Pobłocki J, Drozd A (2025) Dietary Gluten-Free Regimen Does Not Affect the Suppression of the Inflammatory Response in the Arachidonic Acid Cascade in Hashimoto's Disease. Int J Mol Sci 26(13):6507
49. Hu J, Du H, Yuan Y, Guo P, Yang J, Yin X, Liu J, Wu S, Wan J, Gong X (2022) MFG-E8 Knockout Aggravated Nonalcoholic Steatohepatitis by Promoting the Activation of TLR4/NF-κB Signaling in Mice. Mediat Inflamm 2022(1):5791915
50. Cao Y, Yue S, Wang A, Xu L, Hu Y, Qiao X (2022) Antrodia cinnamomea and its compound dehydroeburicoic acid attenuate nonalcoholic fatty liver disease by upregulating ALDH2 activity. Ethnopharmacol 292, 115146. doi: 10.1016, J. JEP

Figures

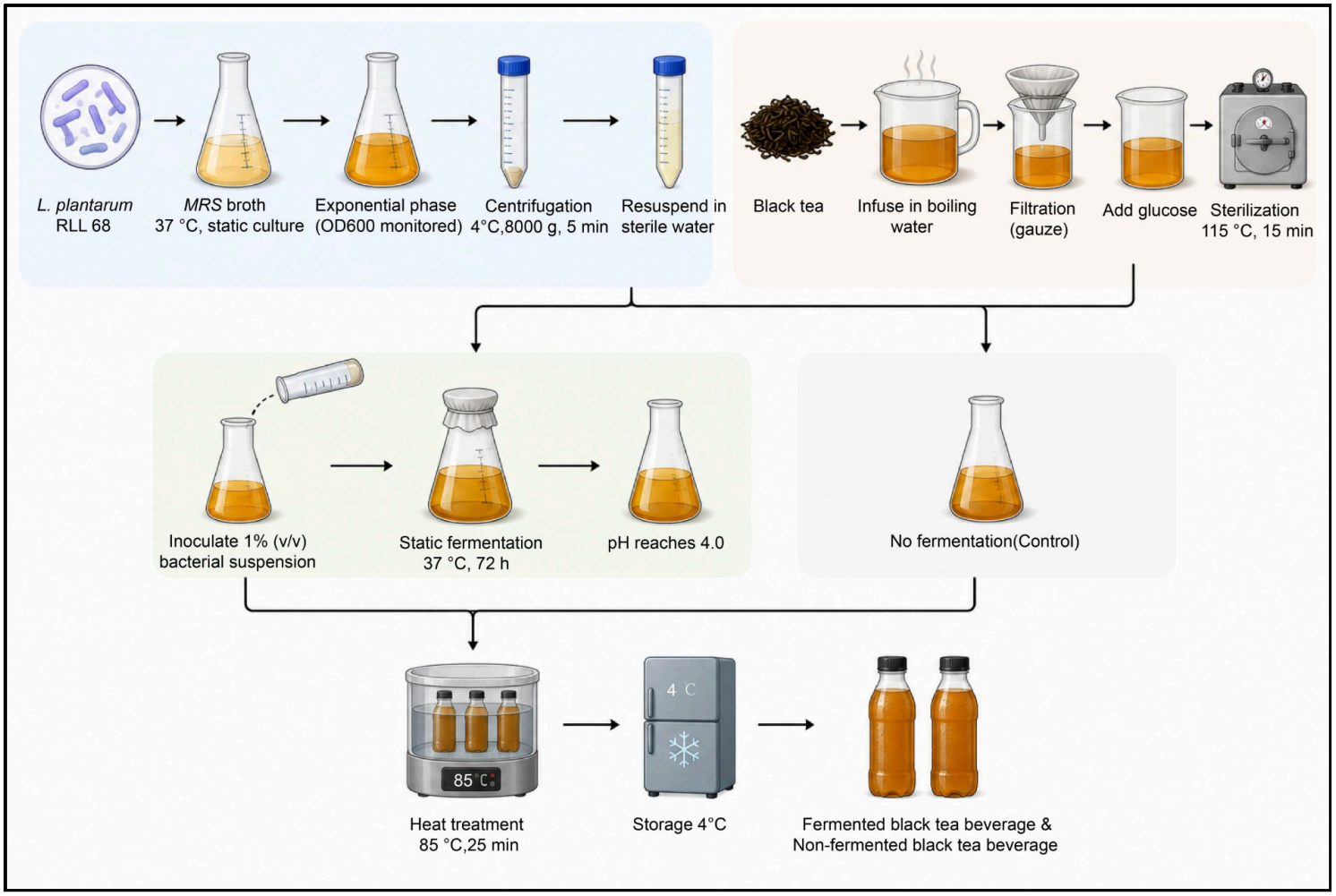


Figure 1

The process flow diagram for the fermentation of black tea beverages by *L. plantarum* RLL68.

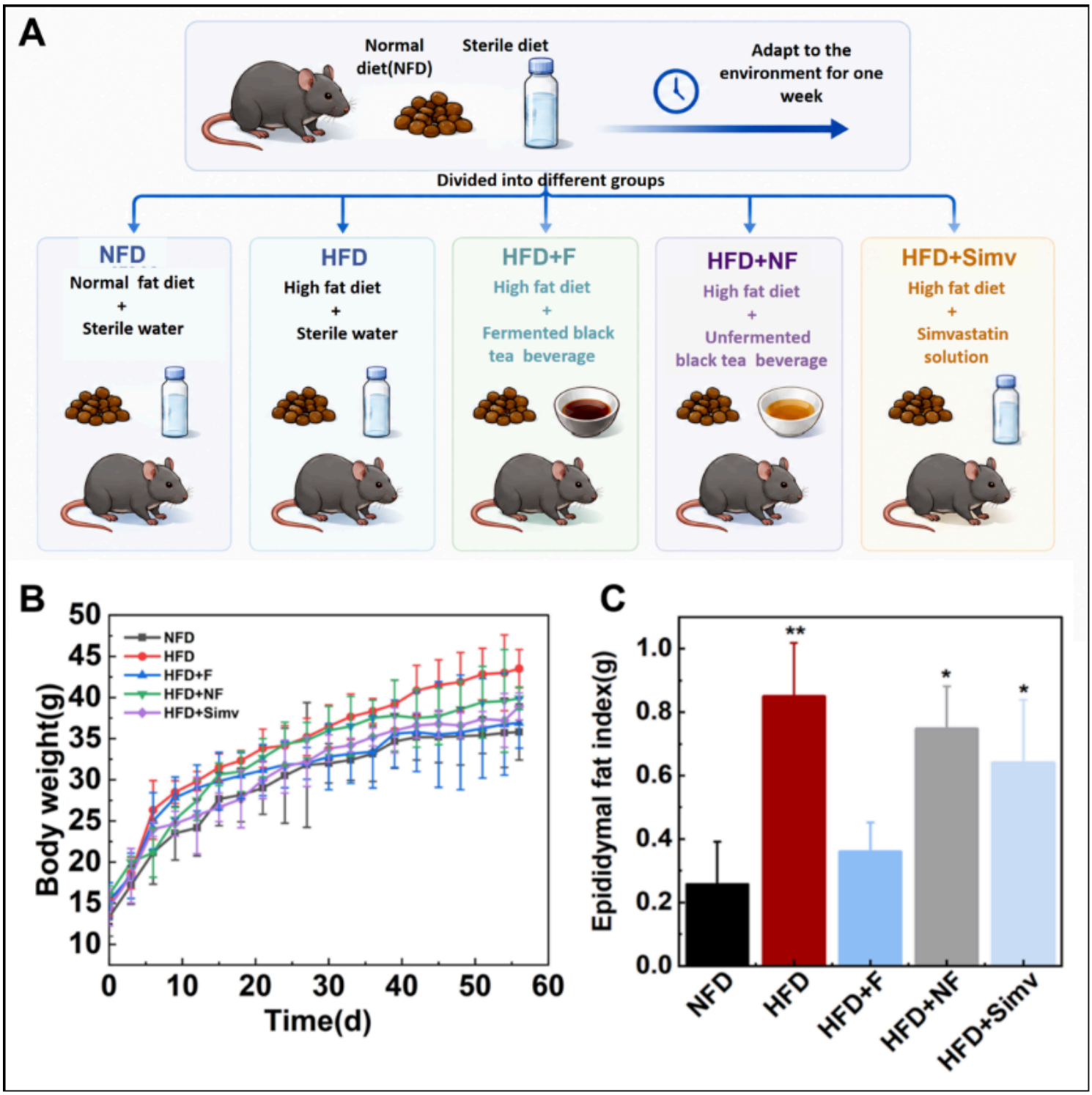


Figure 2

(A) Grouping of animal experiments. (B) The changes in body weight and (C) epididymal fat index of mice in different groups. "*" denotes (P<0.05), and "**" denotes (P<0.01), relative to the NFD group.

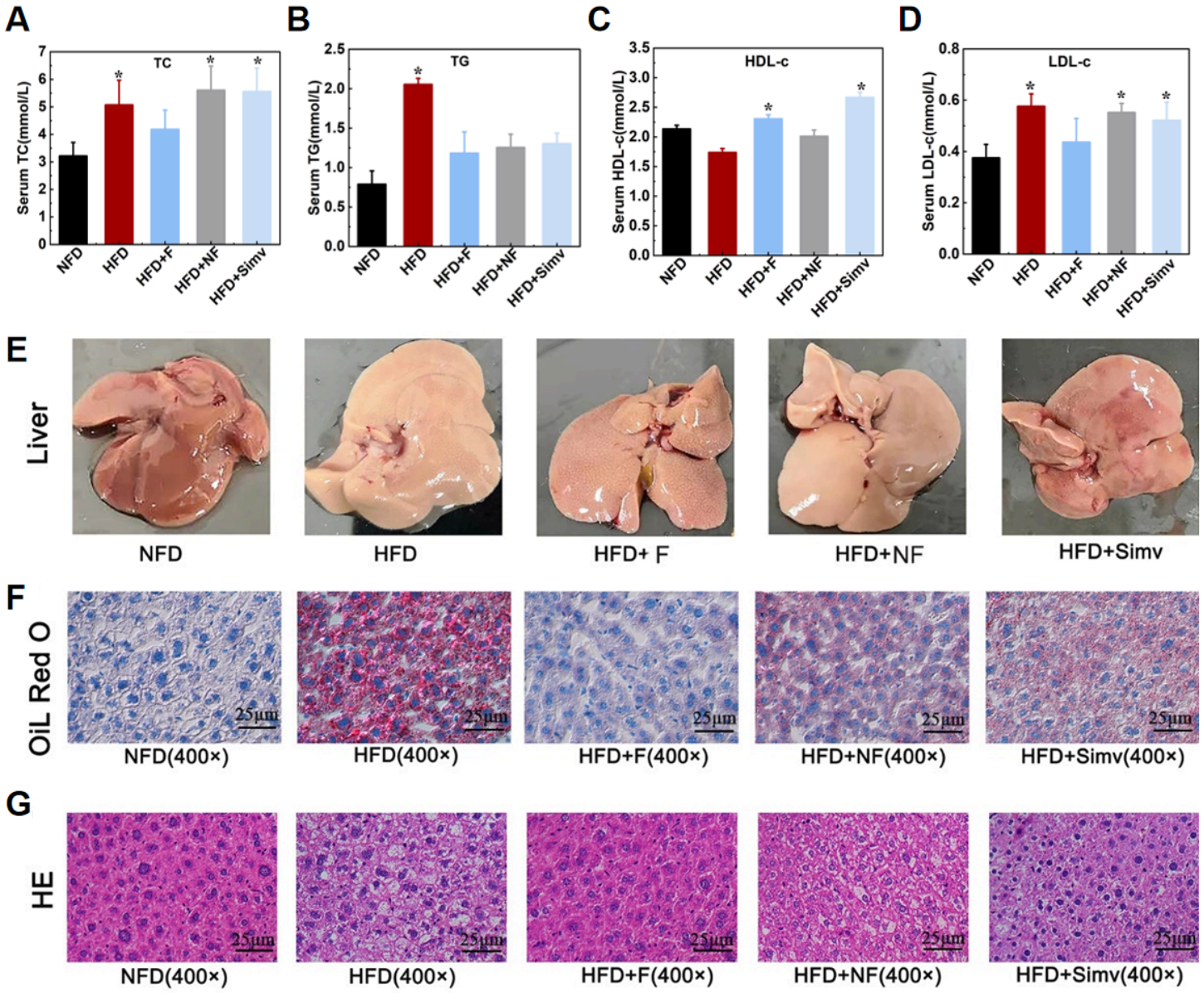


Figure 3

The serum biochemical parameters including (A) TC, (B) TG, (C) HDL and (D) LDL of mice from different experimental groups ("*" denotes (P<0.05), and "**" denotes (P<0.01), relative to the NFD group); (E) Representative photographs of the mice livers in different treatment groups; (F) Representative images of Oil Red O staining and (G) hematoxylin and eosin staining of mice liver tissue sections (original magnification, ×400).

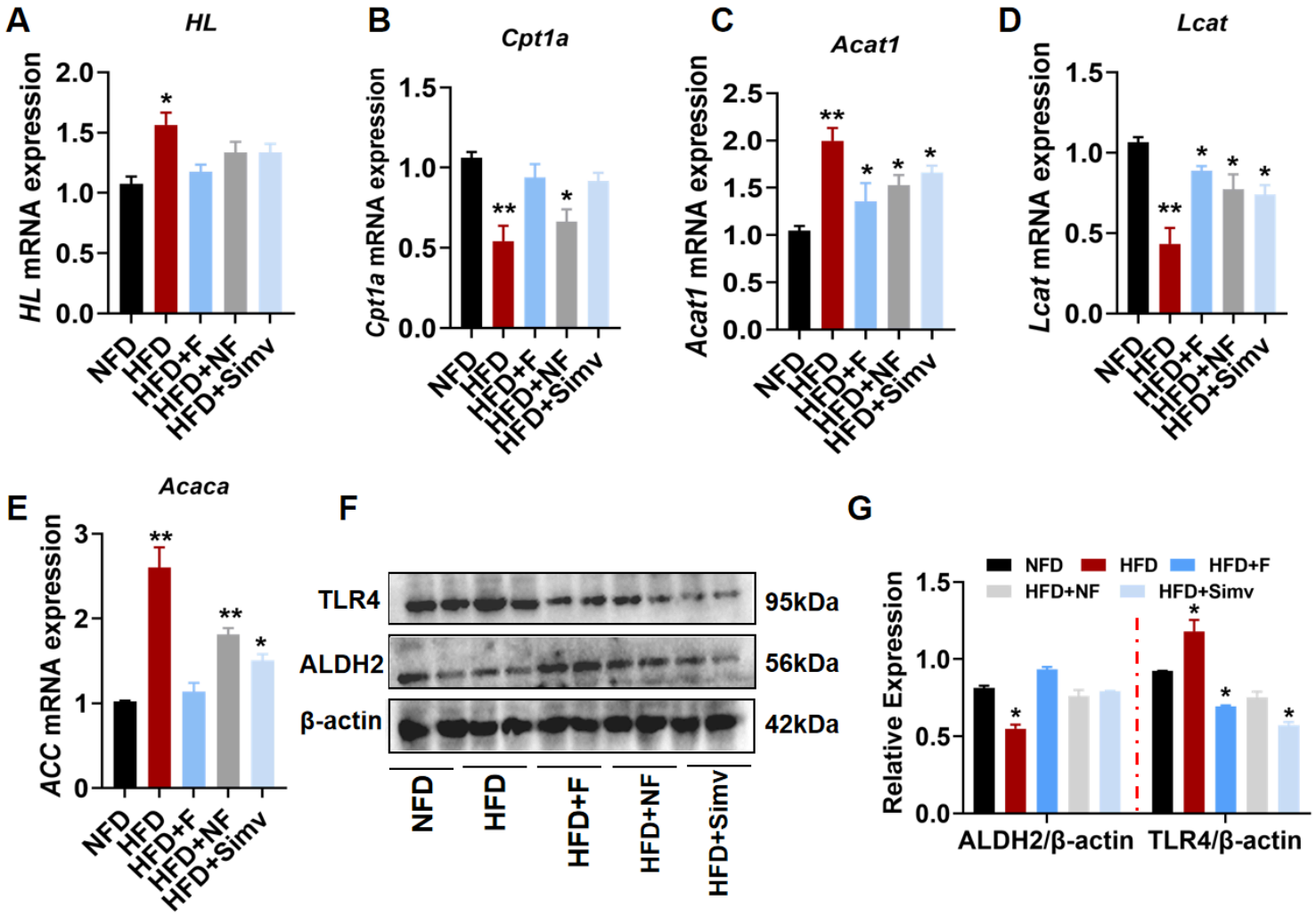


Figure 4

The expression levels of genes associated with lipid metabolism in the liver, including (A) *HL*, (B) *Cpt*1a, (C) *Acat*1, (D) *Lcat*, and (E) *Acaca*, as well as protein expression levels of TLR4 and ALDH2 analyzed by Western Blot (F, G). "*" denotes (P<0.05), and "**" denotes (P<0.01), relative to the NFD group.

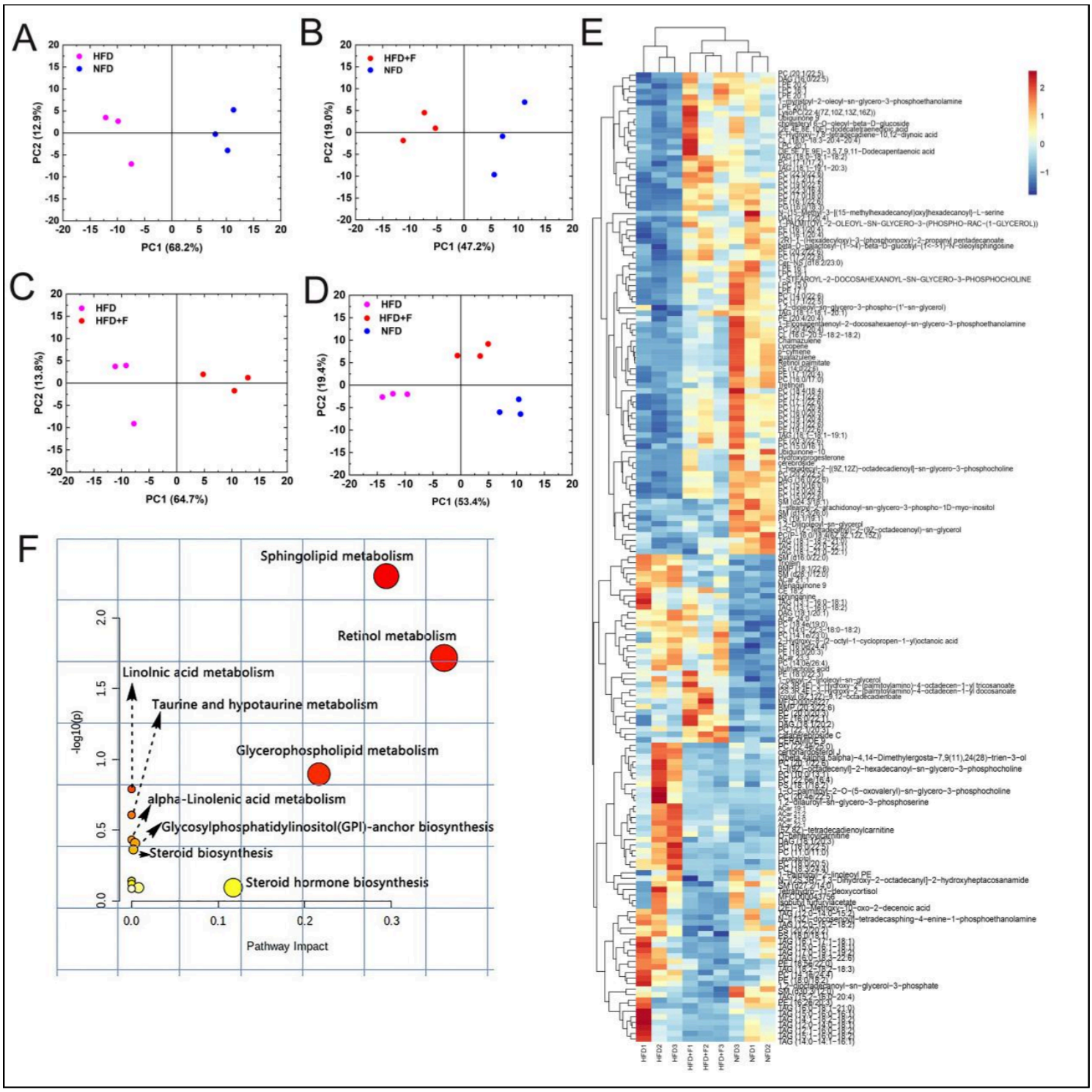


Figure 5

The liver lipid metabolomic profiling by UPLC-QTOF/MS in positive ionization mode (ESI^+). The PCA score plot of liver lipid metabolic profiles of the NFD and HFD groups (A), the NFD and HFD +F groups (B), the HFD and HFD+F groups (C), HFD+F and HFD groups (D). (E) The heatmap of relative abundance of significant different metabolites (VIP > 1.0, and $P < 0.05$) in HFD + F, HFD and NFD groups; (F) The metabolic pathway impact prediction between the HFD and HFD+F groups in liver based on the KEGG

online database. The −log(p) values from the pathway enrichment analysis are indicated on the horizontal axis, and the impact values are indicated on the vertical axis.

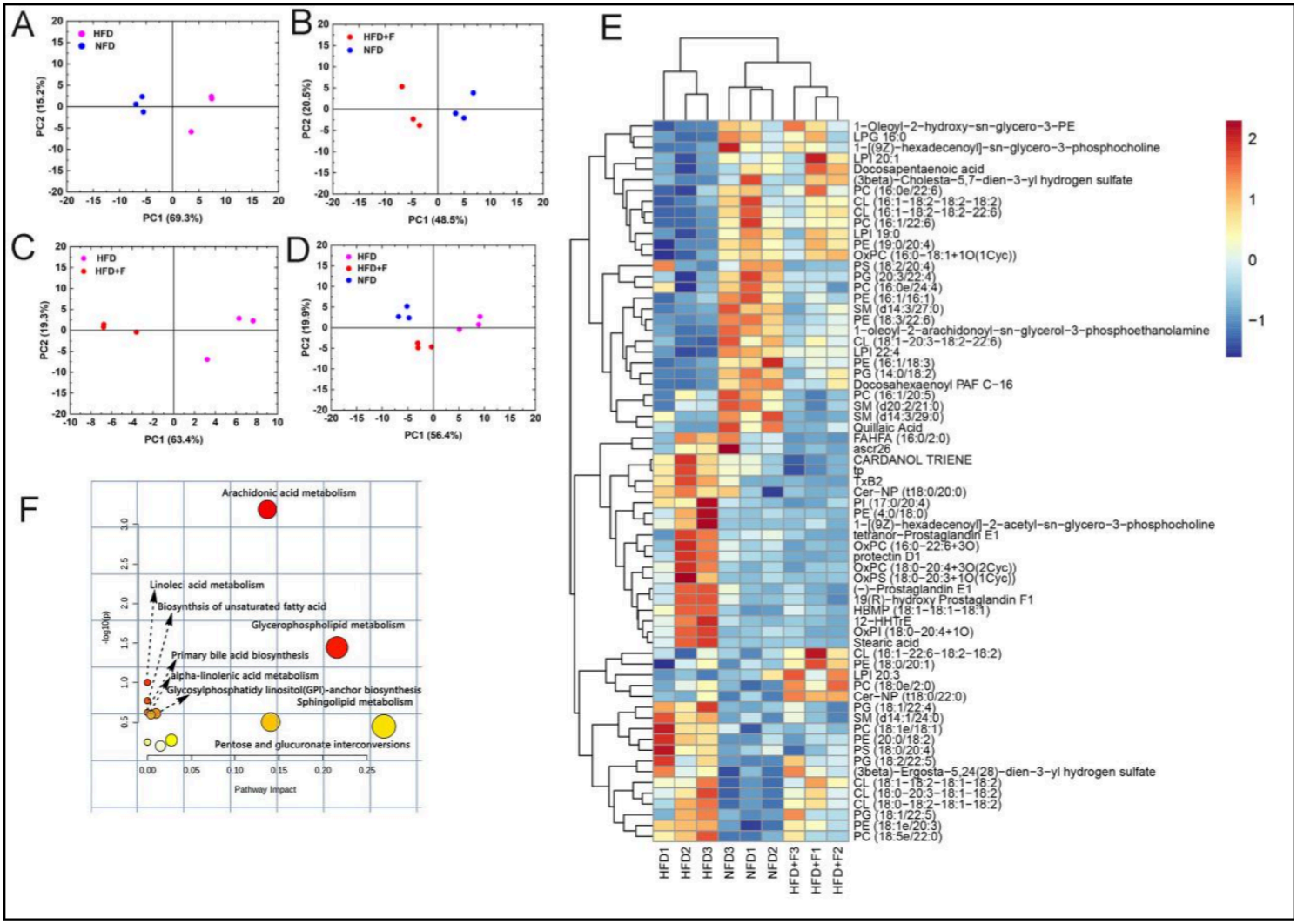


Figure 6

The liver lipid metabolomic profiling by UPLC-QTOF/MS in negative ionization mode (ESI^-). The PCA score plot of liver metabolic profiles of the NFD and HFD groups (A), the NFD and HFD +F groups (B), the HFD and HFD+F groups (C), HFD+F and HFD groups (D). (E) The heatmap of relative abundance of significant different metabolites (VIP > 1.0, and $P < 0.05$) in HFD + F, HFD and NFD groups; (F) The metabolic pathway impact prediction between the HFD and HFD+F groups in liver based on the KEGG online database. The −log(p) values from the pathway enrichment analysis are indicated on the horizontal axis, and the impact values are indicated on the vertical axis.

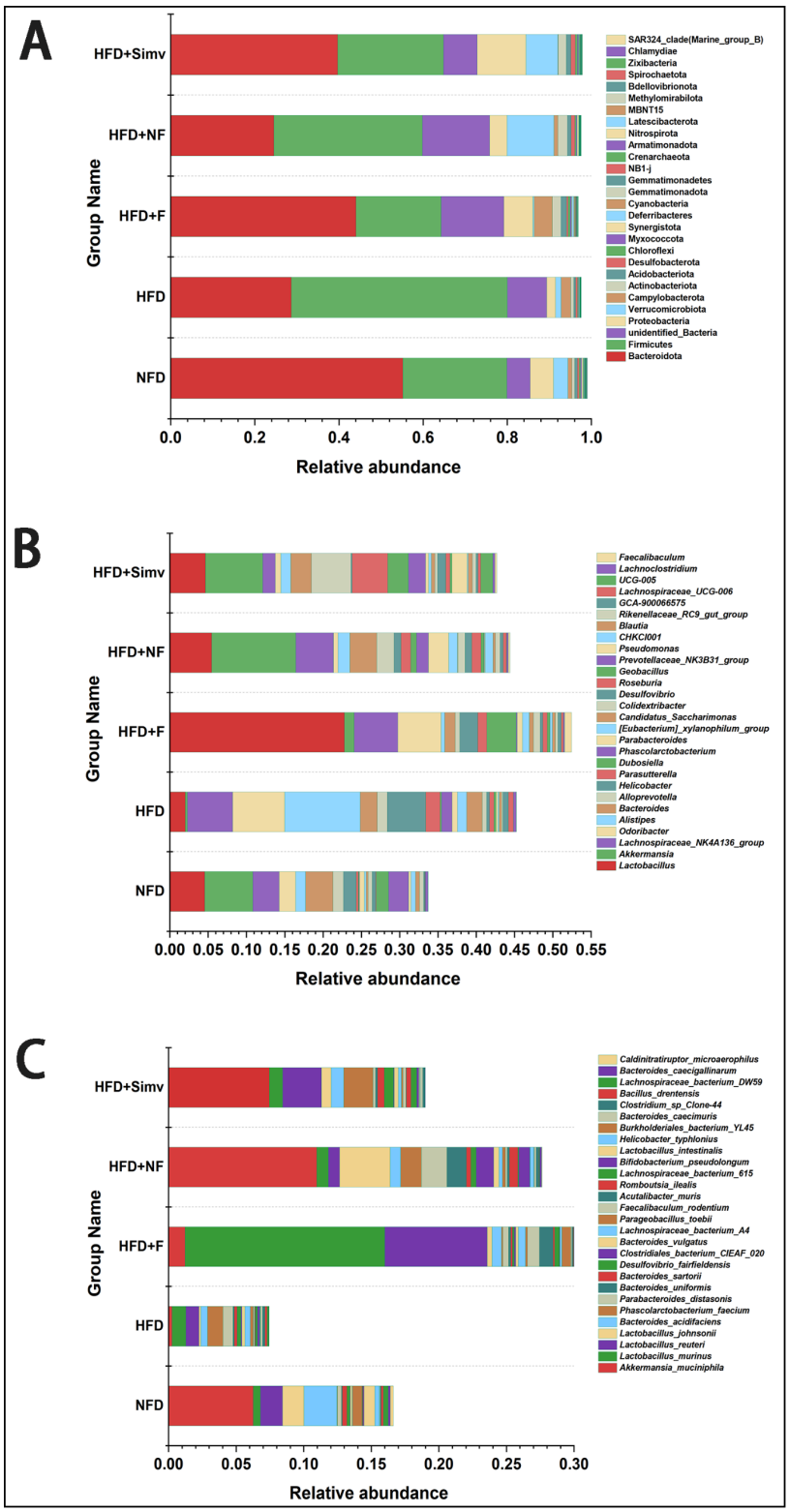


Figure 7

The relative abundance of microbial phyla and genera in the gut microbiota flora of mice across different groups (A: Phylum; B: Genera; C: Species).

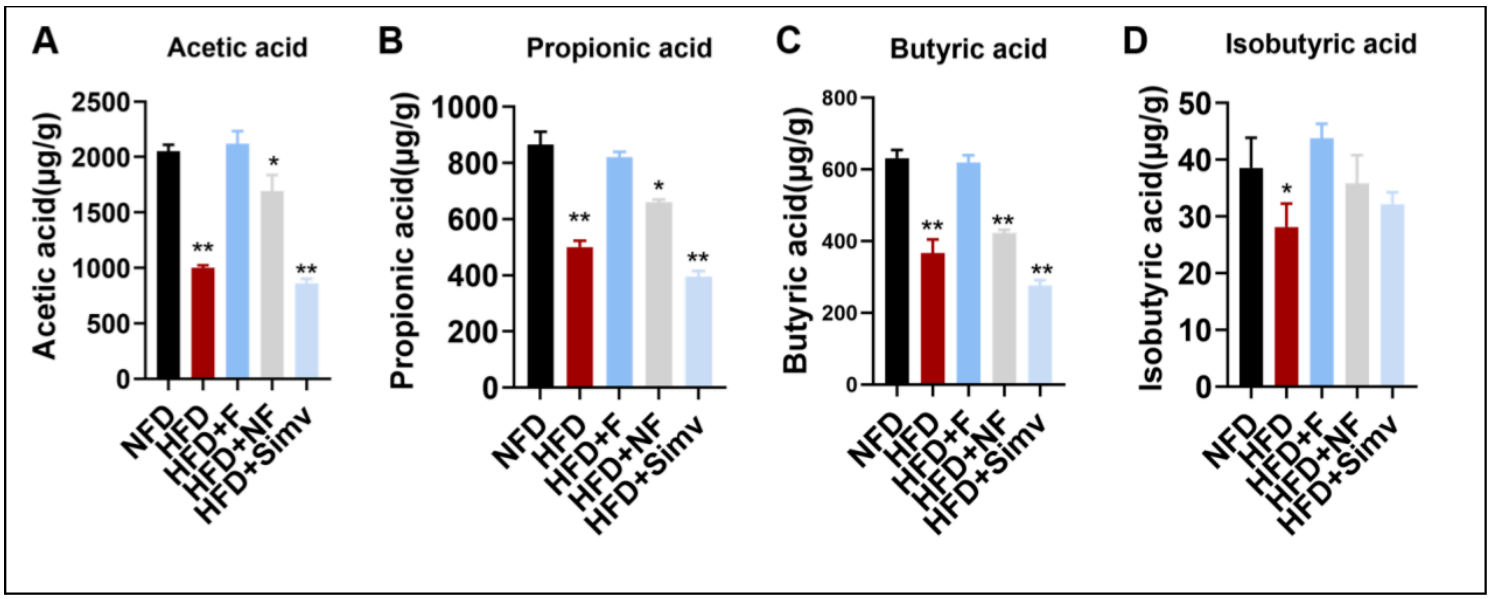


Figure 8

The variation in short-chain fatty acid levels in the faeces of mice. (A) Acetic acid, (B) Propionic acid, (C) Butyric acid, (D) Isobutyric acid. “*” denotes (P<0.05), and “**” denotes (P<0.01), relative to the NFD group.

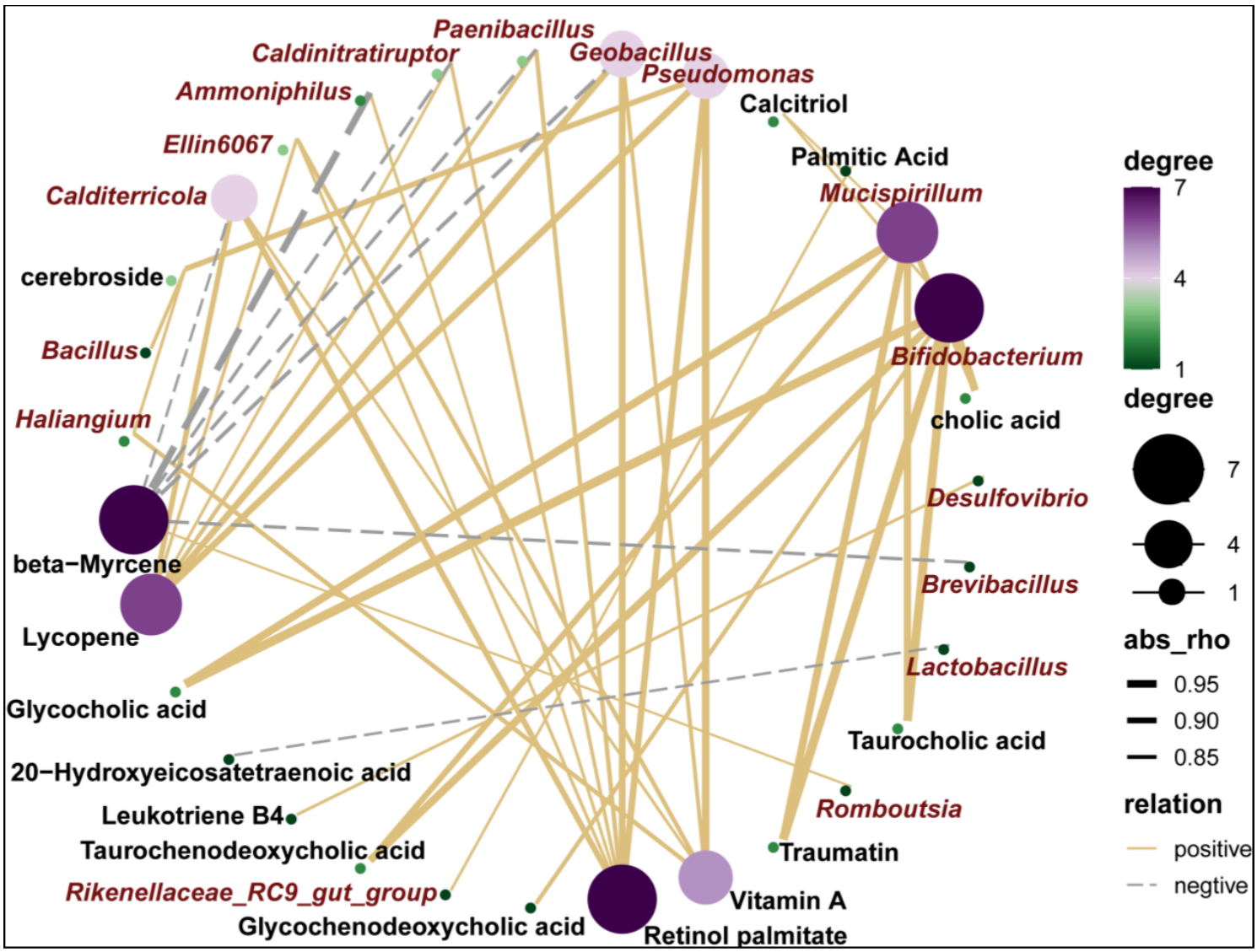


Figure 9

The correlation between key microbiota and lipid metabolic parameters.

Supplementary Files

This is a list of supplementary files associated with this preprint. Click to download.

- Supplementarymaterials.docx